Published in final edited form as:

J Med Chem. 2017 August 24; 60(16): 7186–7198. doi:10.1021/acs.jmedchem.7b00966.

N-(Pivaloyloxy)alkoxy-carbonyl Prodrugs of the Glutamine Antagonist 6-Diazo-5-oxo-L-norleucine (DON) as a Potential Treatment for HIV Associated Neurocognitive Disorders

Michael T. Nedelcovych[†,‡,+], **Lukáš Tenora**[◆,+], **Boe-Hyun Kim**[¶], **Jennifer Kelschenbach**[¶], **Wei Chao**[¶], **Eran Hadas**[¶], **Andrej Jančařík**[◆], **Eva Prchalová**[†,◆], **Sarah C. Zimmermann**[†,‡], **Ranjeet P. Dash**[†], **Alexandra J. Gadiano**[†], **Caroline Garrett**[▽], **Georg Furtmüller**[○], **Byoungchol Oh**[○], **Gerald Brandacher**[○], **Jesse Alt**[†], **Pavel Majer**[*,◆], **David J. Volsky**[*,¶], **Rana Rais**[*,†,‡], and **Barbara S. Slusher**[*,†,‡,§,‖,⊥,#]

[†]Johns Hopkins Drug Discovery, Johns Hopkins School of Medicine, Baltimore, Maryland 21205, United States

[‡]Department of Neurology, Johns Hopkins School of Medicine, Baltimore, Maryland 21205, United States

[§]Department of Medicine, Johns Hopkins School of Medicine, Baltimore, Maryland 21205, United States

[‖]Department of Oncology, Johns Hopkins School of Medicine, Baltimore, Maryland 21205, United States

[⊥]Department of Psychiatry, Johns Hopkins School of Medicine, Baltimore, Maryland 21205, United States

[#]Department of Neuroscience, Johns Hopkins School of Medicine, Baltimore, Maryland 21205, United States

[▽]Department of Molecular and Comparative Pathobiology, Johns Hopkins School of Medicine, Baltimore, Maryland 21205, United States

[*]**Corresponding Authors:** For B.S.S.: phone, 410-614-0662; fax, 410-614-0659; bslusher@jhmi.edu; address, Johns Hopkins Drug Discovery, 855 North Wolfe Street, Baltimore, Maryland 21205, United States. For P.M.: phone, +420-220183125; majer@uochb.cas.cz; address, Institute of Organic Chemistry and Biochemistry, Academy of Sciences of the Czech Republic vvi, Flemingovo nam 2, 166 10 Prague, Czech Republic. For D.J.V.: phone, 212-241-1015; david.volsky@mssm.edu; address, Icahn School of Medicine at Mount Sinai, 1468 Madison Avenue, New York, New York, 10029, United States. For R.R.: phone, 410-502-0497; fax, 410-614-0659; rrais2@jhmi.edu; address, Johns Hopkins Drug Discovery, 855 North Wolfe Street, Baltimore, Maryland 21205, United States.

[+]**Author Contributions**

M.T.N. and L.T. contributed equally

ORCID

Rana Rais: 0000-0003-4059-2453

Barbara S. Slusher: 0000-0001-9814-4157

Notes

The authors declare no competing financial interest.

Supporting Information

The Supporting Information is available free of charge on the ACS Publications website at DOI: 10.1021/acs.jmedchem.7b00966.

Representative chromatogram showing metabolism of **13d** in mouse plasma (PDF)

Molecular formula strings with ex vivo and in vivo metabolism data (CSV)

○Vascularized Composite Allotransplantation Laboratory, Department of Plastic and Reconstructive Surgery Johns Hopkins School of Medicine, Baltimore, Maryland 21205, United States

◆Institute of Organic Chemistry and Biochemistry, Academy of Sciences of the Czech Republic vvi, 166 10 Prague, Czech Republic

¶Department of Medicine, Icahn School of Medicine at Mount Sinai, New York, New York 10029, United States

Abstract

Aberrant excitatory neurotransmission associated with overproduction of glutamate has been implicated in the development of HIV-associated neurocognitive disorders (HAND). The glutamine antagonist 6-diazo-5-oxo-L-norleucine (DON, **14**) attenuates glutamate synthesis in HIV-infected microglia/macrophages, offering therapeutic potential for HAND. We show that **14** prevents manifestation of spatial memory deficits in chimeric EcoHIV-infected mice, a model of HAND. **14** is not clinically available, however, because its development was hampered by peripheral toxicities. We describe the synthesis of several substituted *N*-(pivaloyloxy)alkoxy-carbonyl prodrugs of **14** designed to circulate inert in plasma and be taken up and biotransformed to **14** in the brain. The lead prodrug, isopropyl 6-diazo-5-oxo-2-(((phenyl(pivaloyloxy)methoxy)-carbonyl)amino)hexanoate (**13d**), was stable in swine and human plasma but liberated **14** in swine brain homogenate. When dosed systemically in swine, **13d** provided a 15-fold enhanced CSF-to-plasma ratio and a 9-fold enhanced brain-to-plasma ratio relative to **14**, opening a possible clinical path for the treatment of HAND.

Graphical abstract

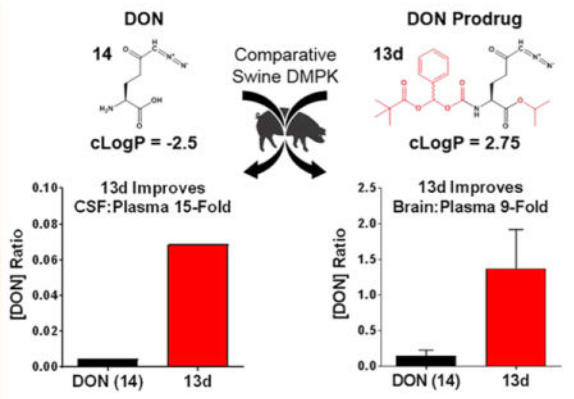

INTRODUCTION

HIV-associated neurocognitive disorders (HAND) remain one of the central health issues in patients with chronic HIV infection[1] despite viremic control by combined antiretroviral therapy (cART).[2] While broad use of cART has markedly reduced the prevalence of HIV-associated dementia (HAD), it has had limited effects on milder forms of HAND which now represent the majority of new cases of HIV neurological disease.[3–5]

Although the mechanisms of HAND pathogenesis are unclear, accumulating evidence suggests that HAND is associated with aberrant glutamate metabolism in the central nervous system (CNS) culminating in elevated extracellular glutamate and disrupted excitatory neurotransmission.[6,7] In cultured human macrophages and microglia, HIV infection induces elevated expression of the glutamate-synthesizing enzyme glutaminase which directly contributes to the toxic overproduction of glutamate.[6,8–19] Activated microglia and macrophages also release viral proteins and pro-inflammatory cytokines[6,7] that independently promote further glutamate synthesis and release[20] and inhibit glutamate reuptake in astrocytes and neurons.[6] These cumulative insults result in impaired glutamate-dependent synaptic function[21–28] and cognition.[25–28]

Studies of HAND patients corroborate preclinical findings of disrupted glutamate metabolism in the CNS. Recent examination of cART-treated HIV patients revealed increased cerebrospinal fluid (CSF) glutamate in patients with HAND compared to those without neurocognitive impairment.[29] Several magnetic resonance spectroscopy (MRS) studies have also shown dysregulated glutamate homeostasis in HIV patients that correlate with neurocognitive impairment including alterations in white and gray matter glutamate and glutamine.[30–35] In addition, microarray analyses in post-mortem brain samples from HAND patients show frontal cortical alterations in the expression of genes critical for the regulation of glutamatergic signaling and glutamate-dependent synaptic plasticity, including glutaminase.[18,36–38]

Collectively, these studies suggest that interventions aimed at normalizing glutamate homeostasis offer therapeutic potential for HAND treatment. The glutamine antagonist 6-diazo-5-oxo-L-norleucine (DON, **14**), which is known to inhibit glutaminase, has been shown to block glutamate over-production induced by HIV infection or immune challenge, and to mitigate excitotoxic neuronal damage both in vitro and in vivo,[13,39–41] but has not yet been tested in an animal model of HAND.

In the present work, we tested the ability of **14** to prevent cognitive decline in EcoHIV-infected wild-type mice which serve as a model of HAND.[42,43] EcoHIV is a chimeric HIV in which the coding region for envelope protein gp120 has been replaced with gp80 from murine leukemia virus, rendering EcoHIV capable of infecting conventional mice.[42] EcoHIV infection results in expression of HIV viral proteins in relevant tissues including microglial cells in the brain[43] and recapitulates many of the neuropathological features of HAND, bolstering the use of these mice as a model system for testing possible HAND therapeutics.[42] We report that when **14** was administered to the mice prior to and during EcoHIV infection, it was able to completely prevent their cognitive decline.

Although exciting, the clinical utility of **14** is limited by its peripheral toxicities mediated primarily by the gastrointestinal (GI) system,[44–46] which is known to be highly glutamine-utilizing. Recently, we described the synthesis of several *N*-(pivaloyloxy)alkoxy-carbonyl **14** prodrugs designed to enhance CNS penetration and brain delivery of **14** while reducing peripheral exposure and thus GI toxicity.[47] Systemic administration in nonhuman primate of one such prodrug, compound **13b**, with isopropyl ester on the carboxylate and *N*-(pivaloyloxy)ethoxy-carbonyl on the amine, resulted in about 10-fold enhancement in the

CSF-to-plasma ratio of **14** exposure relative to administration of equimolar **14**.[47] These findings provided the first evidence that a prodrug strategy could significantly alter the tissue distribution of **14**.

In the current study, we hypothesized that modification of the *N*-(pivaloyloxy)methoxy-carbonyl pro-moiety with additional steric bulk on the methylene bridge could slow peripheral bioconversion of **14** prodrugs and confer further improvement in CNS penetration, as has been shown for other prodrugs utilizing carboxylesterase-mediated hydrolyses.[48–51] In addition to increasing steric hindrance and metabolic stability, our modification approach could also enhance lipophilicity.[52,53] The new **14** prodrugs, compounds **13b**–**e**, with addition of methyl, isopropyl, phenyl, and dimethyl groups to the *N*-(pivaloyloxy)methoxy-carbonyl pro-moiety, respectively, had substantially increased calculated partition coefficients (cLogP) versus **14** (1.50, 2.42, 2.75, and 1.81 vs –2.50, respectively). However, when evaluated in mouse plasma, all of the prodrugs were rapidly and completely metabolized to **14**, precluding attempts to meaningfully differentiate their efficacy/toxicity from **14** in the EcoHIV murine model. Importantly, this conundrum is not uncommon in prodrug discovery, where increased metabolism in rodents is well documented and higher species are necessary to mimic human metabolism.[54,55] Thus, these prodrugs were subsequently tested for stability in human plasma as well as swine, a model organism that closely recapitulates human drug metabolism and pharmacokinetics.[56] Although the *N*-(pivaloyloxy)methoxy-carbonyl derivative of **14**, compound **13a**, was also labile in human and swine plasma, all of the substituted analogues, compounds **13b**–**e**, were found to be metabolically stable. Furthermore, when incubated in homogenates of swine brain, the target tissue for **14** release, compounds **13b** and **13d** were readily converted. These compounds were then tested in vivo in swine. Relative to administration of equimolar **14**, systemic administration of **13b** and **13d** resulted in lower **14** plasma exposure, higher CSF exposure, and a greater than 7- and 15-fold increased CSF-to-plasma ratio, respectively. Having shown the best profile, **13d** and **14** were subsequently assessed in terminal swine studies in which brain levels were directly measured. **13d** afforded a 9-fold enhancement in brain-to-plasma ratio relative to equimolar **14**.

CHEMISTRY

As shown in Scheme 1, the intermediates **4a**–**c** were synthesized by a three-step procedure starting from the appropriate 1-chloroalkyl carbonochloridate (**1a**–**c**), which was reacted with ethanthiol in the presence of triethylamine to yield corresponding *O*-(1-chloroalkyl)-*S*-ethyl carbonothioates (**2a**–**c**). These intermediates were transformed to 1-(((ethylthio)carbonyl)oxy)alkyl pivalate derivatives (**3a**–**c**) by reaction with pivalic acid in the presence of base (DIPEA). Oxidation of the thioester moiety by peracetic acid followed by reaction with *N*-hydroxysuccinimide[57,58] provided **4a**–**c** in a yield of 56–64% after column chromatography (total over three steps). The attempt to use the same methodology for phenyl analogue **13d** in the last step resulted in a complex mixture, likely due to reactivity of the corresponding benzyl cation intermediate. The attempt to prepare the analogous intermediate with a phenyl was unsuccessful. Although it was not confirmed, this

failure could be due to the oxidation of the benzoacetal group by peracetic acid in the third step.

We thus chose to explore the *para*-nitrophenoxy derivative **8**, which can be synthesized via a route devoid of an oxidant as shown in Scheme 2. First, the chloro(phenyl)methyl carbonochloridate (**6**) was prepared by reaction of benzaldehyde (**5**) with triphosgene in the presence of base (pyridine). Intermediate **6** was reacted with 4-nitrophenol to give the chloro(phenyl)methyl (4-nitrophenyl) carbonate (**7**), which was then subjected to reaction with freshly prepared mercury-(II) salt of pivalic acid to yield analogue **8**. Pivalate **8** was then used to prepare **13d** (Scheme 4). Despite several attempts with different pivalates (potassium, silver, palladium) we were not successful in eliminating the use of mercury in this step.

As shown in Scheme 3, compound **11** was prepared in an analogous way. 4-Nitrophenyl prop-1-en-2-yl carbonate (**9**) was prepared from commercially available 2-propenyl chloroformate as previously reported[59] and reacted with hydrogen chloride. The obtained 2-chloropropan-2-yl (4-nitrophenyl) (**10**) was then reacted with mercury(II) pivalate to yield the desired intermediate **11**, which was then used to prepare analogue **13e**.

As shown in Scheme 4, the prodrugs **13a**–**e** were prepared by reaction of **14** isopropyl ester (**12**) with **4a**–**c**, **8**, or **11**, respectively, in dichloromethane (DCM) or dimethylformamide (DMF) at 0 °C or room temperature. Compound **12** was prepared as previously described in detail with yield and purity in agreement with the published data.[47] The compounds **13a**–**e** were obtained in 40–83% yield after purification by liquid chromatography (LC). To improve yields of **13d** and **13e**, an excess of compound **12**[47] and longer reaction time were necessary (see Experimental Section).

RESULTS AND DISCUSSION

Compound 14 Prevented Cognitive Decline, a Major Manifestation of HAND, in EcoHIV-Infected Mice

Similar to HAND patients,[60] mice inoculated with EcoHIV exhibited impaired spatial learning and memory as measured by radial arm water maze (RAWM) 30 days postinfection (Figure 1). EcoHIV infection resulted in a significant increase in the number of errors (Figure 1A) and latency to escape (Figure 1B) onto a hidden platform in the maze. **14** treatment (1 mg/kg, ip, qod) beginning 1 day prior to EcoHIV or sham inoculation and continued throughout the infection period and RAWM testing, fully normalized cognitive performance as measured by both errors (main effect of treatment [$F(3,140) = 261.8$, $p < 0.0001$], trial [$F(4,140) = 146.2$, $p < 0.0001$], interaction [$F(12,140) = 1.93$, $p = 0.0355$]) and latency to escape (main effect of treatment [$F(3,140) = 37.00$, $p < 0.0001$], trial [$F(4,140) = 56.03$, $p < 0.0001$], interaction [$F(12,140) = 1.832$, $p = 0.0484$]). Neither EcoHIV infection nor **14** treatment affected latency to escape to a visible platform (Figure 1C; main effect of trial [$F(3,112) = 34.44$, $p < 0.0001$]), indicating no impairment in visual or motor function. Additionally, no mice exhibited overt signs of toxicity (i.e., diarrhea, weight loss). The EcoHIV-infected mice exhibited measurable viral loads in the spleen and brain (Figure 1D). **14** treatment actually caused an increase in peripheral viral load ($t(14) = 2.58$, $p = 0.022$),

likely due to the well described **14**-mediated inhibition of T cell activity/proliferation,[61,62] which is known to be required for endogenous suppression of EcoHIV replication.[43] Therefore, despite enabling a modest increase in EcoHIV replication, **14** still prevented cognitive decline, suggesting its mechanism of action to be secondary to the infection itself. These findings suggest that glutaminase inhibition through **14** delivery to the CNS prior to or during HIV infection may prevent the development of cognitive impairment in HAND patients.

N-(Pivaloyloxy)alkoxy-carbonyl Prodrugs of 14 Were Synthesized with Improved Lipophilicity

Despite robust efficacy in the EcoHIV model of HAND, the GI toxicity induced by **14** in humans has hampered its clinical development.[44–46] Previous efforts by our group to develop more tolerable prodrugs of **14** yielded compound **13a** (Table 1) through coverage of **14**'s carboxylate and amine groups with isopropyl ester and a primary *N*-(pivaloyloxy)methoxy-carbonyl group, respectively.[47] We rationalized that additional bulky, lipophilic substituents would increase cLogP and further improve CNS penetration. Thus, methyl-, isopropyl-, phenyl-, and dimethyl-analogues of **13a** (compounds **13b**–**e**) were synthesized as described above. cLogP for each of these prodrugs was incrementally and substantially increased relative to **14** (Table 1). We then initiated testing of their ex vivo metabolic stability.

N-(Pivaloyloxy)alkoxy-carbonyl Prodrugs of 14 Were Completely Unstable in Mouse Plasma, Restricting Their Evaluation in Mouse Models

All prodrugs **13a**–**e** were found to be completely metabolized during a 60 min incubation in mouse plasma (Table 1). A representative chromatogram for the rapid metabolism of **13d** in mouse plasma is provided in Supporting Information, Figure S1, showing complete conversion to **14** within 10 min. The rapid metabolism of the **14** prodrugs precluded the examination of their efficacy and toxicity in mice as they would be immediately converted to **14**. As mentioned above, enhanced metabolism in rodents is a common issue with prodrugs of various classes,[54,55] necessitating the use of higher species, such as swine, that more closely model human metabolism.[56]

N-(Pivaloyloxy)alkoxy-carbonyl Prodrugs of 14 Were Stable in Human and Swine Plasma but Labile in Brain Homogenate

Consistent with previous reports of the metabolic lability of *N*-(pivaloyloxy)methoxy-carbonyl group-containing prodrugs,[47–51,63] compound **13a** was found to be rapidly metabolized during a 60 min incubation in human plasma (Table 1). In contrast, we found that modification of **13a** with methyl-, isopropyl-, phenyl-, and dimethyl- substitutions (**13b**–**e**) resulted in a significant improvement in human plasma stability (Table 1). As our goal was to evaluate these prodrugs in an animal model which mimicked human metabolism, we next tested the stability of compounds **13b**–**e** in swine plasma. We found that all of the prodrugs, similar to human plasma, were stable in swine plasma (Table 1). Given that the target compartment for **14** activity in HAND is the brain, **13b**–**e** were then tested for metabolic lability in swine brain homogenate. Compounds **13c** and **13d** were

found to be readily biotransformed in swine brain homogenate, whereas **13b** was moderately labile and **13e** was mostly stable (Figure 2). Swine brain homogenate half-lives were calculated for each compound and found to be significantly different from each other [$F(3,8) = 31.42$, $p < 0.0001$].

When Tested in Swine, Compounds 13b and 13d Resulted in Enhanced 14 CSF-to-Plasma Ratios; Compound 13d Showed an Optimal Profile

To determine if the ex vivo metabolism data translated in vivo, **14**, **13b**, and **13d** were selected for pharmacokinetic evaluation in swine. Consistent with their observed metabolic stability, iv infusion of **13b** and **13d** (1.6 mg/kg **14** equivalent dose) resulted in 3–5-fold lower **14** plasma exposures relative to an equimolar dose of **14** (Figure 3A). Plasma AUC_{0-t} for **14**, **13b**, and **13d** were 29.9, 8.00, and 5.70 nmol·h/mL, respectively. The opposite trend occurred in CSF, where the prodrugs delivered substantially higher amounts of **14** to the CSF (Figure 3B; Table 2), resulting in significantly increased CSF-to-plasma ratios (Figure 3C; Table 3). The improvement over **14** in CNS penetration correlated with the lipophilicity of each prodrug. The cLogP for **13d** was nearly twice that calculated for **13b** (2.75 vs 1.50) and was associated with a doubling of the improvement in CSF-to-plasma ratio in vivo (approximately 15-fold increase for **13d** vs 7-fold increase for **13b** relative to equimolar **14**). These experiments confirm that POM-based ester prodrugs substantially improve CNS delivery of **14** and support the hypothesis that iterative derivatization of this promoiety with sterically hindering, lipophilic residues promotes better CNS targeting. It should be noted that the **13b** diastereomers were separable by standard column chromatography,[47] whereas the **13d** diastereomers were not readily separable by the same method and thus were administered as a mixture. This may not influence the clinical relevance of these findings, as human plasma stabilities of the **13b** diastereomers were comparable (91% vs 89% remaining at 60 min for **13b-1** and **13b-2**, respectively).[47] However, as **13d** moves toward clinical development, stereochemical purity will be prioritized.

In Terminal Swine Studies, Compound 13d Resulted in Enhanced 14 Brain-to-Plasma Ratio

Because CSF is not always an accurate surrogate for brain concentrations, we conducted terminal studies in swine with the lead compound **13d** where plasma and brain tissue were collected. At 60 min postinfusion of **13d** (1.6 mg/kg **14** equivalent dose), **14** delivery to the plasma was substantially lower than equimolar **14** (Figure 4A) while brain levels were comparable (Figure 4B; Table 2). This resulted in a 9-fold enhancement in the brain-to-plasma ratio of **13d** relative to equimolar **14** (Figure 4C), similar to its enhanced CSF-to-plasma ratio (Table 3). Given that the **14** CSF levels were significantly lower than that observed in brain tissues, we next conducted protein binding studies in an attempt to elucidate the reason for these differences. Plasma protein binding of **14** was low (F_b = 21%), consistent with previous reports.[46] However, higher brain protein binding of **14** was observed (F_b= 91%), providing a possible explanation for the CSF and brain level discrepancies. On the basis of this value, free levels of **14** in the swine brain were calculated to be 0.531 nmol/g at 60 min postadministration of **13d**, closer to observed levels of **14** delivered to the CSF by **13d** at the same time point (~1.0 nmol/mL; Table 2).

CONCLUSION

14 was robustly efficacious in preventing cognitive decline in EcoHIV-infected mice used as a model of HAND. However, **14** is not suitable for clinical use due to its dose-limiting peripheral toxicities. To translate these findings to the clinic, we describe the synthesis of several substituted *N*-(pivaloyloxy)alkoxy-carbonyl prodrugs of **14** that improve CNS penetration. Rational design of **14** prodrugs by addition of lipophilic substituents to the *N*-(pivaloyloxy)alkoxy-carbonyl pro-moiety yielded sterically hindered compounds with increased metabolic stability in swine and human plasma, favorable conversion in brain homogenate, and substantially improved CNS delivery in vivo in swine, exemplified by compound **13d**. Metabolic stability of these prodrugs in human plasma was very similar to that observed in swine, suggesting strong translational potential for this strategy. This approach may therefore enable the clinical use of brain glutaminase inhibition for the treatment of HAND and other neuropsychiatric disorders characterized by aberrant glutamate metabolism.

EXPERIMENTAL SECTION

The commercially available HPLC grade acetonitrile, catalysts, and reagent grade materials were used as received. TLC was performed on Silica gel 60 F254-coated aluminum sheets (Merck), and spots were detected by the solution of $Ce(SO_4)_2.4H_2O$ (1%) and $H_3P(Mo_3O_{10})_4$ (2%) in sulfuric acid (10%). Flash chromatography was performed on Silica Gel 60 (0.040–0.063 mm, Fluka) or on Biotage KP-C18-HS or KP-Sil SNAP cartridges using the Isolera One HPFC system (Biotage, Inc.). All chemicals were purchased from Sigma-Aldrich or TCI and were used without further purification. The ^{1}H NMR spectra were measured at 400.1 MHz and ^{13}C NMR spectra at 100.8 MHz. For standardization of ^{1}H NMR spectra, the internal signal of TMS (δ 0.0, $CDCl_3$) or residual signals of $CDCl_3$ (δ 7.26) were used. In the case of ^{13}C NMR spectra, the residual signal of $CDCl_3$ (δ 77.00) was used. The chemical shifts are given in δ scale; the coupling constants J are given in Hz. The ESI mass spectra were recorded using ZQ micromass mass spectrometer (Waters) equipped with an ESCi multimode ion source and controlled by MassLynx software. Alternatively, the low resolution ESI mass spectra were recorded using a quadrupole orthogonal acceleration time-of-flight tandem mass spectrometer (Q-Tof Micro, Waters) and high resolution ESI mass spectra using a hybrid FT mass spectrometer combining a linear ion trap MS and the Orbitrap mass analyzer (LTQ Orbitrap XL, Thermo Fisher Scientific). The conditions were optimized for suitable ionization in the ESI Orbitrap source (sheat gas flow rate 35 au, aux gas flow rate 10 au of nitrogen, source voltage 4.3 kV, capillary voltage 40 V, capillary temperature 275 °C, tube lens voltage 155 V). The samples were dissolved in methanol and applied by direct injection. The purity of all compounds subjected to biological testing was established using HPLC (Jasco Inc.) equipped with a Reprosil 100 C18, 5 μm, 250 mm × 4 mm column. The analysis was performed using a gradient of 2% CH_3CN/98% H_2O with 0.1% TFA → 100% CH_3CN, with UV detection, λ = 210 nm. Purity of all compounds subjected to biological testing was over 95%. Optical rotations were measured in $CHCl_3$ using an Autopol IV instrument (Rudolph Research Analytical). IR spectra were measured in $CHCl_3$ on an FT-IR spectrometer.

((((2,5-Dioxopyrrolidin-1-yl)oxy)carbonyl)oxy)methyl Pivalate (4a)

Chloromethyl carbonochloridate **1a** (2.00 g, 1.38 mL, 15.5 mmol) was dissolved in anhydrous Et_2O (20 mL). The reaction mixture was cooled to 0 °C, and the mixture of Et_3N (1.57 g, 2.16 mL, 15.5 mmol, 1 equiv) and EtSH (964 mg, 1.15 mL, 15.5 mmol, 1 equiv) in anhydrous Et_2O (5 mL) was added dropwise over 5 min. The resulting mixture was then stirred overnight (25 h) at rt. Precipitate was filtered through a pad of Celite, and solvent was removed under reduced pressure. The crude *O*-(chloromethyl) *S*-ethyl carbonothioate **2a** (2.4 g, colorless liquid) was used in the next step without purification. **2a** (2.40 g, 15.5 mmol) was dissolved in pivalic acid (9.51 g, 93.1 mmol, 6 equiv), and freshly prepared salt of pivalic acid (4.76 g, 46.6 mmol, 3 equiv) and DIPEA (6.02 g, 8.10 mL, 46.6 mmol, 3 equiv) were added in few portions. The reaction mixture was heated to 60 °C for 22 h. EtOAc (100 mL) was added, and the organic phase was extracted with water (100 mL), satd $NaHCO_3$ (3 × 100 mL), and satd NaCl (100 mL), dried over $MgSO_4$, solvent was removed under reduced pressure, and the crude product **3a** (3.30 g, 97%, light-yellow liquid) was used in the next step without purification. (((Ethylthio)-carbonyl)oxy)methyl pivalate **3a** (3.20 g, 14.5 mmol) was dissolved in anhydrous DCM (40 mL), *N*-hydroxysuccinimide (3.34 g, 29.1 mmol, 2 equiv) was added, and the suspension was cooled to 0 °C. Peracetic acid (3.31 g (100%), 9.21 g (36%), 43.6 mmol, 3 equiv, 36% solution in acetic acid) was added dropwise over 15 min. The resulting mixture was stirred for 1 h at 0 °C and 2 h at rt. DCM (50 mL) was added, and the organic phase was washed with water (30 mL) and satd NaCl (30 mL), dried over $MgSO_4$, solvent was removed under reduced pressure, and column chromatography of the residue (EtOAc/hexane 1:2, R_f 0.27) yielded **4a** as a colorless solid (2.54 g, 64% over three steps). ^{1}H NMR (400 MHz, $CDCl_3$): δ 1.24 (9H, s), 2.84 (4H, s), 5.86 (2H, s). ^{13}C NMR (101 MHz, $CDCl_3$): δ 25.56 (2C), 26.86 (3C), 38.96, 83.67, 150.90, 168.34 (2C), 176.54. IR ($CHCl_3$): 2979 m, 2939 w, 2876 w, 1823 s, 1796 vs, 1649 vs, 1481 m, 1463 m, 1456 w, 1431 m, 1398 w, 1371 m, 1367 m, 1280 m, 1199 vs, 1110 vs, 1047 m, 998 s, 986 s, 942 m, sh, 924 s, 853 w, cm^{-1}. ESI MS: 296 ($[M + Na]^+$). HR ESI MS: calcd for $C_{11}H_{15}O_7NNa$ 296.07407; found 296.07410.

((((2,5-Dioxopyrrolidin-1-yl)oxy)carbonyl)oxy)ethyl Pivalate (4b)

Chloroethyl carbonochloridate **1b** (2.00 g, 1.51 mL, 14.1 mmol) was dissolved in anhydrous Et_2O (20 mL). The reaction mixture was cooled to 0 °C, and the mixture of Et_3N (1.43 g, 1.97 mL, 14.1 mmol, 1 equiv) and EtSH (876 mg, 1.02 mL, 14.1 mmol, 1 equiv) in anhydrous Et_2O (5 mL) was added dropwise over 5 min. The resulting mixture was then stirred overnight (17 h) at rt. Precipitate was filtered through a pad of Celite, and solvent was removed under reduced pressure. The crude *O*-(1-chloroethyl) *S*-ethyl carbonothioate **2b** (2.20 g, colorless liquid) was used in the next step without purification. **2b** (2.20 g, 13.1 mmol) was dissolved in pivalic acid (8.02 g, 78.6 mmol, 6 equiv), and freshly prepared salt of pivalic acid (4.01 g, 39.3 mmol, 3 equiv) and DIPEA (5.08 g, 6.85 mL, 39.3 mmol, 3 equiv) was added in few portions. The reaction mixture was heated to 70 °C for 20 h. EtOAc (100 mL) was added, and the organic phase was extracted with water (100 mL), satd $NaHCO_3$ (3 × 100 mL), and satd NaCl (100 mL), dried over $MgSO_4$, solvent was removed under reduced pressure, and the crude product **3b** (2.82 g, 92%, light-yellow liquid) was used in the next step without purification. (((Ethylthio)carbonyl)oxy)methyl pivalate **3b**

(2.82 g, 12.1 mmol) was dissolved in anhydrous DCM (40 mL), *N*-hydroxysuccinimide (2.77 g, 24.1 mmol, 2 equiv) was added, and the suspension was cooled to 0 °C. Peracetic acid (2.76 g (100%), 7.67 g (36%), 36.3 mmol, 3 equiv, 36% solution in acetic acid) was added dropwise over 15 min. The resulting mixture was stirred for 1 h at 0 °C and 2 h at rt. DCM (50 mL) was added, and the organic phase was washed with water (30 mL) and satd NaCl (30 mL), dried over $MgSO_4$, solvent was removed under reduced pressure, and column chromatography of the residue (EtOAc/hexane 1:2, R_f 0.27) yielded **4b** as a colorless oil (2.02 g, 50% over three steps). ^{1}H NMR (400 MHz, $CDCl_3$): δ 1.21 (9H, s), 1.60 (3H, d, J = 5.4), 2.83 (4H, s), 6.81 (1H, q, J = 5.4). ^{13}C NMR (101 MHz, $CDCl_3$): δ 19.43, 25.58 (2C), 6.88 (3C), 38.89, 93.83, 150.01, 168.43, 176.10. IR ($CHCl_3$): 2978 m, 2939 w, 2875 w, 1821 s, 1795 s, 1748 vs, br, 1480 m, 1432 m, 1396 m, 1371 m, 1365 m, sh, 1298 w, sh, 1280 s, 1199 s, 1054 vs, 1028 s, 944 vw, sh, 935 w, sh, 811 w, cm^{-1}. ESI MS: 310 ([M + Na]$^+$). HR ESI MS: calcd for $C_{12}H_{17}O_7NNa$ 310.08972; found 310.08979.

1-((((2,5-Dioxopyrrolidin-1-yl)oxy)carbonyl)oxy)-2-methylpropyl Pivalate (4c)

1-Chloro-2-methylpropyl carbonochloridate **1c** (2.00 g, 1.71 mL, 11.7 mmol) was dissolved in anhydrous Et_2O (20 mL). The reaction mixture was cooled to 0 °C, and the mixture of Et_3N (1.18 g, 1.63 mL, 11.7 mmol) and EtSH (727 mg, 866 μL, 11.7 mmol) in anhydrous Et_2O (10 mL) was added dropwise over 10 min. The resulting mixture was stirred overnight (23 h) at rt. Precipitate was filtered through a pad of Celite, and solvent was removed under reduced pressure. The crude product *O*-(1-chloro-2-methylpropyl) *S*-ethyl carbonothioate **2c** (2.20 g, 96%, colorless liquid) was used in the next step without purification. **2c** (1.20 g, 6.10 mmol) was dissolved in pivalic acid (3.74 g, 4.20 mL, 36.6 mmol, 6 equiv), and freshly prepared salt of pivalic acid (1.87 g, 2.10 mL, 18.3 mmol, 3 equiv) and DIPEA (2.37 g, 3.19 mL, 18.3 mmol, 3 equiv) were added in few portions. The reaction mixture was heated to 60 °C for 70 h. EtOAc (100 mL) was added, and the organic phase was extracted with water (50 mL), satd $NaHCO_3$ (3 × 50 mL), satd NaCl (50 mL), dried over $MgSO_4$, solvent was removed under reduced pressure, and the crude product 1-(((ethylthio)carbonyl)oxy)-2-methylpropyl pivalate **3c** (1.32 g, 83%, light-yellow liquid) was used in the next step without purification. **3c** (1.28 g, 4.88 mmol) was dissolved in anhydrous DCM (13 mL), *N*-hydroxysuccinimide (1.12 g, 9.76 mmol, 2 equiv) was added, and the suspension was cooled to 0 °C. Peracetic acid (1.11 g (100%), 3.09 g (36%), 14.6 mmol, 3 equiv, 36% solution in acetic acid) was added dropwise over 10 min. The resulting mixture was stirred for 1 h at 0 °C and for 2 h at rt. DCM (40 mL) was added, and the organic phase was washed with water (20 mL) and satd NaCl (20 mL), dried over $MgSO_4$, solvent was removed under reduced pressure, and column chromatography of the residue (EtOAc/hexane 3:5, R_f 0.26) yielded **4c** as a light-yellow oil (863 mg, 56% over 3 steps). ^{1}H NMR (400 MHz, $CDCl_3$): δ 1.00 (6H, d, J = 6.9), 1.21 (9H, s), 2.08–2.19 (1H, m), 2.81 (4H, s), 6.55 (1H, d, J = 5.0). ^{13}C NMR (101 MHz, $CDCl_3$): δ 16.06, 16.38, 25.55, 26.89, 31.84, 39.05, 98.19, 150.37, 168.48, 176.14. IR ($CHCl_3$): 2978 m, 2938 w, 2878 w, 1821 s, 1795 s, 1748 vs, br, 1481 m, 1463 w, 1432 m, 1396 w, 1373 m, 1366 m, sh, 1279 m, 1199 s, 1046 m, 998 m, sh, 987 m, 932 s cm^{-1}. ESI MS: 338 ([M + Na]$^+$). HR ESI MS: calcd for $C_{14}H_{21}O_7NNa$ 338.12102; found 338.12115.

Chloro(phenyl)methyl(4-nitrophenyl)carbonate (7)

Chloro-(phenyl)methyl carbonochloridate (**6**) was prepared from benzaldehyde (**5**) by a previously reported method.[64] Compound **6** (900 mg, 4.39 mmol) was dissolved in anhydrous DCM (20 mL), 4-nitrophenol (611 mg, 4.39 mmol, 1 equiv) was added, and the mixture was cooled to 0 °C. Pyridine (347 mg, 355 μL, 4.39 mmol, 1 equiv) in anhydrous DCM (5 mL) was added dropwise over 5 min. Reaction mixture was stirred for 2 h at rt. DCM was evaporated, and the crude product was purified by column chromatography (DCM/hexane 1:1). Compound **7** was obtained as a colorless solid (520 mg, 39%). ^{1}H NMR (400 MHz, $CDCl_3$): δ 7.33 (1H, s), 7.41–7.50 (5H, m), 7.58–7.63 (2H, m), 8.28–8.34 (2H, m). ^{13}C NMR (101 MHz, $CDCl_3$): δ 87.37, 121.83 (2C), 125.59 (2C), 126.41 (2C), 129.07 (2C), 130.56, 136.35, 145.91, 150.50, 155.07. IR ($CHCl_3$): 3119 w, 3088 w, 3071 vw, 3032 w, 1788 vs, 1772 s, sh, 1619 m, 1595 m, 1530 vs, 1492 s, 1456 m, 1349 vs, 1317 m, 1296 m, 1232 vs, sh, 1178 m, sh, 1165 m, 1111 m, 1105 w, sh, 1078 m, 1054 s, 1029 m, 1014 m, 1002 w, 978 s, 920 w, 872 s, 854 s, 830 vw, 708 s, 695 m, sh, 680 w, 626 vw, 618 vw, 530 vw, 495 w, 403 w cm^{-1}. ESI MS: 329 ($[M + Na]^+$). HR ESI MS: calcd for $C_{14}H_{10}O_5NClNa$ 330.01397; found 330.01367.

(((4-Nitrophenyloxy)carbonyl)oxy)(phenyl)methyl Pivalate (8)

Compound **7** (100 mg, 0.325 mmol) and mercury pivalate (157 mg, 0.390 mmol, 1.2 equiv) were dissolved in anhydrous DCM (6 mL). Reaction mixture was stirred under inert atmosphere at rt overnight (16 h). DCM (10 mL) was added, and reaction mixture was washed with satd $NaHCO_3$ (10 mL) and brine (10 mL), the organic phase was dried over $MgSO_4$, and DCM was evaporated. The product **8** (115 mg, 95%) was used in the next step without purification. ^{1}H NMR (400 MHz, $CDCl_3$): δ 1.28 (9H, s), 7.38–7.43 (2H, m), 7.44–7.50 (3H, m), 7.57–7.60 (1H, m), 7.61 (1H, s), 8.23–8.33 (2H, m). ^{13}C NMR (101 MHz, $CDCl_3$): δ 27.02 (3C), 39.11, 93.80, 121.86 (2C), 125.47 (2C), 126.84 (2C), 128.97 (2C), 130.48, 134.39, 145.69, 150.73, 155.32, 176.44. IR ($CHCl_3$): 3118 w, 3087 w, 3072 w, 3031 m, 2980 m, 2875 w, 1775 vs, 1747 s, 1618 m, 1595 m, 1529 vs, 1493 s, 1480 m, 1459 m, 1399 m, 1365 m, 1349 vs, 1279 vs, 1248 vs, 1165 s, 1123 vs, 1112 s, sh, 1030 s, 1014 m, 1003 m, 970 s, br, 943 s, 918 m, 865 s, 860 s, 832 w, 697 s, 682 w, 633 w, 619 vw, 530 vw, 495 w, 403 vw cm^{-1}. ESI MS: 396 ($[M + Na]^+$). HR ESI MS: calcd for $C_{19}H_{19}O_7NNa$ 396.10537; found 396.10546.

2-(((4-Nitrophenyloxy)carbonyl)oxy)propan-2-yl Pivalate (11)

2-Chloropropan-2-yl (4-nitrophenyl) carbonate **10**[59] (300 mg, 1.16 mmol) was dissolved in anhydrous DCM (15 mL). Mercury pivalate (559 mg, 1.39 mmol, 1.2 equiv) was added, and the reaction mixture was stirred overnight (20 h) at rt under inert atmosphere. The solid precipitate ($HgCl_2$) was removed by filtration, DCM (15 mL) was added, and organic phase was washed with satd $NaHCO_3$ (15 mL) and satd NaCl (15 mL), dried over $MgSO_4$, solvent was removed under reduced pressure, and the product **11** was obtained as a light-yellow oil (301 mg, 80%). ^{1}H NMR (400 MHz, $CDCl_3$): δ 1.20 (9H, s), 1.91 (6H, s), 7.34–7.40 (2H, m), 8.24–8.30 (2H, m). ^{13}C NMR (101 MHz, $CDCl_3$): δ 25.28 (2C), 27.02 (3C), 39.59, 107.71, 121.98 (2C), 125.40 (2C), 145.50, 149.07, 155.41, 175.97. IR ($CHCl_3$): 3031 w, 2976 w, 2875 w, 1777 m, 1736 m, 1618 w, 1595 w, 1528 m-s, 1493 m, 1481 w, 1439 w,

1396 w, 1376 w, 1349 m, 1322 w, 1264 m, 1191 m, 1112 vs, 1094 s, sh, 1030 w, 980 w, 859 m, 682 vw, 491 vw cm^{-1}. ESI MS: 348 ($[M + Na]^+$). HR ESI MS: calcd for $C_{15}H_{19}O_7NNa$ 348.10537; found 348.10543.

Isopropyl 6-Diazo-5-oxo-2-((((pivaloyloxy)methoxy)-carbonyl)amino)hexanoate (13a)

Compound **4a** (320 mg, 1.17 mmol) was suspended in anhydrous DCM (6 mL). The reaction mixture was cooled to 0 °C, and compound **12**[47] (250 mg, 1.17 mmol, 1 equiv) in anhydrous DCM (3 mL) was added dropwise. The mixture was stirred for 15 min at 0 °C and then 2 h at rt. Solvent was removed under reduced pressure, and column chromatography of the residue (EtOAc/hexane 1:2, R_f 0.21) yielded the desired compound **13a** (175 mg, 40%) as yellow oil. ^{1}H NMR (400 MHz, $CDCl_3$): δ 1.19 (9H, s), 1.23 (3H, d, J = 6.2), 1.24 (3H, d, J = 6.2), 1.90–2.05 (1H, m), 2.14–2.25 (1H, m), 2.31–2.51 (2H, m), 4.28 (1H, td, J = 8.2, 4.7), 5.03 (1H, hept, J = 6.2), 5.27 (1H, bs), 5.65 (1H, d, J = 8.1), 5.69 (1H, d, J = 5.7), 5.73 (1H, d, J = 5.7). ^{13}C NMR (101 MHz, $CDCl_3$): δ 21.79, 21.81, 26.97, 36.34, 38.86, 53.63, 54.90, 69.75, 80.33, 154.40, 171.01, 177.51, 193.43. Optical rotation: $[\alpha]^{22}_D$ +13.0° (c 0.184, $CHCl_3$). IR ($CHCl_3$): 3424 m, 3354 w, br, 3116 w, 2984 s, 2937 m, 2875 s, 2110 vs, 1747 vs, 1730 vs, sh, 1642 s, 1512 s, 1481 m, 1466 m, 1453 m, 1377 s, 1282 s, 1182 m, 1145 s, 1105 s, 994 s, 942 m, cm^{-1}. ESI MS: 394 ($[M + Na]^+$). HR ESI MS: calcd for $C_{16}H_{25}O_7N_3Na$ 394.15847; found 394.15855.

Isopropyl 6-Diazo-5-oxo-2-(((1-(pivaloyloxy)ethoxy)-carbonyl)amino)hexanoate (13b)

This compound was prepared according to a procedure previously described in detail.[47] Yields and ^{1}H NMR and ^{13}C NMR spectra were in agreement with the published data.

Isopropyl 6-Diazo-2-(((2-methyl-1-(pivaloyloxy)propoxy)-carbonyl)amino)-5-oxohexanoate (13c)

Compound **4c** (399 mg, 1.27 mmol, 0.9 equiv) was suspended in anhydrous DCM (7 mL). The reaction mixture was cooled to 0 °C, and compound **12**[47] (300 mg, 1.41 mmol, 1 equiv) in anhydrous DCM (3 mL) was added dropwise. The mixture was stirred for 15 min at 0 °C and then 2 h at rt. Solvent was removed under reduced pressure, and column chromatography of the residue (EtOAc/hexane 1:2, R_f 0.30) yielded **13c** (285 mg, 54%) as yellow oil (mixture of two stereoisomers 1:1). ^{1}H NMR (400 MHz, $CDCl_3$, first stereoisomer): δ 0.94 (6H, d, J = 6.8), 1.16 (9H, s), 1.23 (6H, t, J = 6.3), 1.83–2.50 (4H, m), 4.22–4.31 (1H, m), 5.02 (1H, hept, J = 6.8), 5.29 (1H, bs), 5.48 (1H, d, J = 8.3), 6.52 (1H, d, J = 4.9). ^{13}C NMR (101 MHz, $CDCl_3$, first stereoisomer): δ 16.40, 16.54, 27.00, 28.05, 31.87, 36.29, 38.96, 53.38, 54.82, 69.64, 94.21, 154.28, 171.31, 176.56, 193.87. ^{1}H NMR (400 MHz, $CDCl_3$, second stereoisomer): δ 0.93 (6H, d, J = 6.8), 1.18 (9H, s), 1.22 (6H, t, J = 6.3), 1.83–2.50 (4H, m), 4.22–4.31 (1H, m), 5.00 (1H, sept, J = 6.8), 5.37 (1H, bs), 5.45 (1H, d, J = 8.3), 6.48 (1H, d, J = 4.9). ^{13}C NMR (101 MHz, $CDCl_3$, second stereoisomer): δ 16.37, 16.54, 26.98, 27.74, 31.91, 36.55, 38.92, 53.54, 54.82, 69.66, 93.87, 154.22, 171.17, 176.81, 193.58. Optical rotation: $[\alpha]^{22}_D$ +11.5° (c 0.261, $CHCl_3$). IR ($CHCl_3$): 3428 m, 3116 w, 2982 s, 2936 m, 2878 m, 2110 vs, 1741 vs, br, 1731 vs, sh, 1641 s, 1508 s, 1480 m, 1463 m, 1400 m, sh, 1385 s, sh, 1377 s, 1365 s, sh, 1281 s, 1231 s, 1183 m, 1146 s, 1105 s,

990 s, 941 m cm^{-1}. ESI MS: 436 ($[M + Na]^+$). HR ESI MS: calcd for $C_{19}H_{31}O_7N_3Na$ 436.20542; found 436.20553.

Isopropyl 6-Diazo-5-oxo-2-(((phenyl(pivaloyloxy)methoxy)-carbonyl)amino)hexanoate (13d)

Compound **8** (817 mg, 2.19 mmol) was dissolved in anhydrous DMF (15 mL). Compound **12**[47] (700 mg, 3.18 mmol, 1.5 equiv) in anhydrous DMF (7 mL) was added dropwise. Reaction mixture was stirred at rt under inert atmosphere for 5 h. DMF was evaporated, and column chromatography of the residue (EtOAc/hexane 1:2, R_f 0.18) yielded product **13d** (648 mg, 66%) as a light-yellow oil (mixture of two stereoisomers 1:1). ^{1}H NMR (400 MHz, $CDCl_3$): δ 1.17–1.31 (15H, m), 1.90–2.06 (1H, m), 2.12–2.31 (1H, m), 2.31–2.54 (2H, m), 4.27–4.36 (1H, m), 5.03 (1H, hept, J = 6.3), 5.29 (1H, bs), 5.59 (1H, d, J = 8.1), 7.36–7.42 (3H, m), 7.46–7.51 (2H, m), 7.61 (s, 1H). ^{13}C NMR (101 MHz, $CDCl_3$): δ 21.82 (2C), 26.99 (3C), 27.70, 36.35, 38.99, 53.55, 54.90, 69.79, 90.93, 126.57 (2C), 128.66 (2C), 129.64, 135.95, 153.82, 171.10, 176.33, 193.51. Optical rotation: $[\alpha]^{22}_D$ +12.5° (c 0.246, $CHCl_3$). IR ($CHCl_3$): 3425 w, 3116 w, 3098 vw, 3070 vw, 3029 m, 2984 m, 2937 m, 2875 w, 2110 s, 1735 vs, br, 1641 s, 1590 w, 1507 s, 1480 m, 1457 m, 1398 m, 1377 s, 1367 s, sh, 1366 s, sh, 1280 s, 1182 m, 1146 s, sh, 1133 s, 1105 s, 1085 m, 1057 s, 1027 s, 1003 m, 942 m, 918 w, 697 m, 619 vw cm^{-1}. ESI MS: 470 ($[M + Na]^+$). HR ESI MS: calcd for $C_{22}H_{29}O_7N_3Na$ 470.18977; found 470.18985.

Isopropyl 6-Diazo-5-oxo-2-((((2-(pivaloyloxy)propan-2-yl)-oxy)carbonyl)amino)hexanoate (13e)

Compound **11** (936 mg, 2.88 mmol) was dissolved in anhydrous DMF (18 mL), and the reaction mixture was cooled to 0 °C. Compound **12**[47] (920 mg, 4.32 mmol, 1.5 equiv) in anhydrous DMF (6 mL) was added dropwise. Reaction mixture was stirred at 0 °C under inert atmosphere for 5 h. DMF was evaporated, and column chromatography of the residue (EtOAc/hexane 1:2, R_f 0.22) yielded product **13e** (955 mg, 83%) as a light-yellow oil. ^{1}H NMR (400 MHz, $CDCl_3$): δ 1.19 (9H, s), 1.23 (3H, d, J = 6.3), 1.24 (3H, d, J = 6.3), 1.80 (3H, s), 1.83 (3H, s), 1.90–2.01 (1H, m), 2.14–2.27 (1H, m), 2.29–2.51 (2H, m), 4.24 (1H, dt, J = 8.3, 4.7), 5.05 (1H, hept, J = 6.3), 5.31 (1H, bs), 5.44 (1H, d, J = 8.2). ^{13}C NMR (101 MHz, $CDCl_3$): δ 21.80, 21.82, 25.76, 25.91, 27.07 (3C), 27.79, 36.46, 39.48, 53.26, 54.87, 69.59, 105.44, 153.16, 171.31, 176.21, 193.63. Optical rotation: $[\alpha]^{22}_D$ +12.8° (c 0.133, $CHCl_3$). IR ($CHCl_3$): 3430 w, 3116 w, 2984 m, 2936 m, 2874 m, 2110 s, 1732 vs, br, 1641 m, 1502 s, 1481 m, 1466 m, 1462 m, 1455 m, 1452 m, 1397 m, sh, 1384 s, 1374 s, 1365 s, sh, 1198 s, 1184 s, 1147 m, sh, 1128 s, 1112 s, 1105 s, 1045 m, 942 w cm^{-1}. ESI MS: 329 ($[M + Na]^+$). HR ESI MS: calcd for $C_{18}H_{29}O_7N_3Na$ 422.18977; found 422.18982.

EcoHIV-Infected Mice

All mouse efficacy studies were conducted in full compliance with NIH guidelines and with the approval of the Institutional Animal Care and Use Committee at the Icahn School of Medicine at Mount Sinai. Male C57BL/6J mice at 5 weeks old (The Jackson Laboratory, Bar Harbor, ME) were maintained on a 12 h light–dark cycle with ad libitum access to food and water. EcoHIV chimeric virus was generated by transfecting HEK293T cells with plasmid DNA containing the EcoHIV construct, specifically EcoNDK containing the V5C5

fragment of gp120.[42] EcoHIV was then collected from the culture media, concentrated by centrifugation, and titered by p24 ELISA (Advanced Biosciences Laboratory, Rockville, MD). Each mouse was randomized to begin **14** (1 mg/kg, ip, qod) or saline treatment 1 day prior to inoculation with either EcoHIV (2×10^6 pg p24, ip) or sham inoculation with PBS ($n = 8$/group) as previously described.[65] The dose of **14** was chosen based on several published efficacy studies in CNS models including multiple sclerosis,[66] brain cancer,[47] and sindbus virus[62,67,68] as well as our lab's mouse pharmacokinetic studies showing μM brain levels of **14** after 1 mg/kg systemic dosing.[69] On day 30 postinoculation (p.i.), having allowed time for stable virus infection and emergence of cognitive deficits, all mice began behavioral training and testing.

Radial Arm Water Maze

The radial arm water maze (RAWM) test was administered in a pool of opaque water containing six swimming lanes and a hidden platform with visual cues essentially as described.[70] The visual cues consisted of both two- and three-dimensional objects that were affixed to the side of the maze pool using clear packing tape. The two-dimensional cues were six different brightly colored 8½ × 11 sheets of paper each printed with a different black shape (square, triangle, star, etc.), and the three-dimensional cues were commonly found laboratory items (funnel, culture flask, pipet tip box, etc.). Briefly, RAWM consisted of four learning trials (LT) of 60 s and one post-training 60 s retention test (RT) administered after 30 min rest every day until test completion. Testing was considered complete when control mice reached asymptotic performance of one error or fewer in finding the hidden platform on trials LT4 and RT. Errors for the last 3 days of testing for all groups were then averaged and used for statistical analysis. The hidden platform was rotated randomly to a different arm each test day to ensure that mice used working memory to locate the platform. Each of the training trials began by placing a mouse randomly into one of the six swimming arms and allowing the mouse to swim for 60 s to find the hidden platform, during which time the number of errors (entering an arm without the platform and/or 20 s of immobility) and latency to locate the hidden platform were recorded. The retention test was performed in the same manner as the learning trials. The hidden platform tests were followed by measuring the latency it took for treated and control mice to find a visible platform in the same context, as a control for possible effects of treatment on animal vision, motivation, or ability to swim to the platform.

Viral Load

After completion of behavioral testing, all mice were sacrificed by carbon dioxide asphyxiation after brief isoflurane anesthesia. Spleen and brain were harvested, DNA was isolated, and viral load was measured as previously described.[65,71–73] Briefly, total DNA was isolated from mouse tissues by sequentially homogenizing in Trizol, mixing with DNAzol, precipitating with ethanol, washing, and treating with NaOH. Quantitative PCR (qPCR) was then conducted to detect EcoHIV/NDK DNA from the *gag* gene region using Taqman chemistry with MGB probes with forward primer 5′-TGGGACCACAGGCTACACTAGA-3′, reverse primer 5′-CAGCCAAAACTCTTGCTTTATGG-3′, and probe 5′-TGATGACAGCATGCCAGGGAGTGG-3′ (ThermoFisher Scientific). A standard curve for

quantitation of copy number was constructed using graded numbers of a plasmid containing the EcoNDK *gag* amplicon. Copy number was then normalized to cell count by amplification of murine *gapdh* (Mm99999915_g1). All qPCR amplification was performed in an Applied Biosystems 7500 instrument.

In Vitro Metabolic Stability

Metabolic stability of prodrugs were evaluated as previously described.[47] Briefly, prodrugs (10 μM) were spiked in mouse, swine, and human plasma or swine brain homogenate and incubated in each matrix in an orbital shaker at 37 °C. Relative prodrug amounts at 0 and 60 min for plasma and 0, 30, and 60 min for brain were measured using liquid chromatography and tandem mass spectrometry (LC–MS/MS) by removing 100 μL aliquots of each mixture in triplicate and quenching each reaction by addition of three times the volume of ice-cold acetonitrile spiked with the internal standard (losartan 5 μM). The samples were vortexed for 30 s and centrifuged at 12000g for 10 min. Then 50 μL of each supernatant was diluted with 50 μL of water and transferred to a 250 μL polypropylene vial sealed with a Teflon cap. Prodrug detection was performed on a Thermo Scientific Accela UPLC system coupled to Accela open autosampler on an Agilent C18 (100 mm × 2.1 mm i.d.) UPLC column. The autosampler was temperature controlled and was operated at 10 °C. The mobile phase used for the chromatographic separation was composed of acetonitrile/water containing 0.1% formic acid and flow rate of 0.5 mL/min for 4.5 min using gradient elution. The column effluent was monitored using TSQ Vantage triple-quadrupole mass-spectrometric detector, equipped with an electrospray probe set in the positive ionization mode. Samples were introduced into the ionization source through a heated nebulized probe (350 °C). Relative prodrug amounts were measured from ratio of peak areas of analyte to IS; percent remaining was calculated by normalizing this value at 60 min to the value obtained at 0 min.

Protein Binding

The free **14** fraction (f_u) in swine plasma and swine brain homogenate was determined using a previously described ultrafiltration method.[74] Briefly, the **14** (10 μM) spiked plasma and/or brain homogenate was incubated at 37 °C for 30 min, following which the samples were loaded onto an ultrafiltration column tube (Corning Spin-X UF with a MW cut off of 30 kDa), whose base is impermeable to the plasma and brain proteins. The samples were centrifuged for 45 min at 37 °C and 4000 rpm (1800*g*). The concentrations were determined in both the filtrate and plasma before filtration, following extraction and quantified via LC-MS/MS. Fraction unbound was calculated from the equation $C_u/C_t \times 100$, where C_u was the concentration in the ultrafiltrate and C_t was the concentration in the plasma or brain homogenate prior to filtration.

In Vivo Pharmacokinetics

Swine studies were conducted under a protocol approved by the Johns Hopkins Animal Care and Use Committee. Adult, female Göttingen × Yucutan miniature swine (Massachusetts General Hospital, MA) were housed in Johns Hopkins University facilities accredited by the Association for Assessment and Accreditation of Laboratory Animal Care International in compliance with the Animal Welfare Act, Animal Welfare Regulations, and the Public

Health Service Policy on the Humane Care and Use of Laboratory Animals. Animals were maintained on a 14 h light and 10 h dark schedule, and provided ad libitum water and a commercial miniswine diet (Teklad, Madison, WI) with environmental enrichment (fruit/vegetables) twice daily. Animals were individually housed while on study in order to monitor behavior and clinical health following drug administration. Whole blood for drug pharmacokinetic evaluation was collected from a dual lumen central venous catheter (CVC) implanted in the external jugular vein prior to study initiation. Animals were anesthetized with a combination of ketamine hydrochloride (20–30 mg/kg, im) and xylazine (2 mg/kg, im), intubated, and maintained under isoflurane (1–2%) inhalant anesthesia. A temporary peripheral saphenous vein catheter was placed in the hind limb to allow for anatomical separation of drug infusion and whole blood sampling via CVC. **14**, **13b**, or **13d** were dissolved in a sterile saline solution containing 5% ethanol and 5% Tween 80 prior to iv infusion via saphenous vein catheter over 1 h (1 mL/min) for a final dose of 1.6 mg/kg or molar equivalent administered at 1 mL/kg (n = 1/dose). Blood samples (1 mL) were taken from CVC at predose, 5, 15, 30, 45, and 60 min. Plasma was separated by low speed centrifugation at 3000g for 10 min at 4 °C. CSF was obtained from the cisterna magna using a 3.5 in. × 22 gauge spinal needle (Becton Dickinson Health Care, Franklin Lakes, New Jersey, USA) at 60 min postdose. All samples were flash frozen upon harvest and stored at –80°C until bioanalysis.

In a separate study, the above dosing procedure was repeated except that the animals (n = 2/dose) were euthanized at 60 min postinfusion using Euthasol (Virbac Animal Health, Fort Worth, TX, USA) containing pentobarbital sodium and phenytoin sodium at a dose of 1 mL per 10 lbs of body weight and plasma and brain tissues were harvested. To obtain brain tissues, a horizontal incision connecting both orbits was extended toward the base of the ears and skin, and subcutaneous tissue over the swine skull were removed. A reciprocating saw was used to cut through the frontal aspect of the calvarium to create a window for intracranial access. Next, the dura mater was cut and a 2 cm × 2 cm sample of full thickness frontal cortex was obtained. All samples were flash frozen and stored at –80 °C until bioanalysis.

Bioanalysis

Quantitation of **14** in plasma, CSF, and brain homogenate by LC-MS/MS was performed as previously described.[47] Briefly, **14** was extracted from plasma, CSF, and brain samples with methanol containing glutamate-d_5 (10 μM ISTD) by vortexing followed by centrifugation 16000g for 5 min. Supernatants were aliquoted and dried at 45 °C for under vacuum for 1 h. Sodium bicarbonate buffer (0.2M, pH 9.0) and dabsyl chloride (10 mM) in acetone were added to each tube, mixed, and incubated for 15 min at 60 °C to derivatize. Samples were then injected and separated on an Agilent 1290 equipped with an Agilent Eclipse plus C18 RRHD 2.1 mm × 100 mm column over a 2.5 min gradient from 20 to 95% acetonitrile +0.1% formic acid and quantified on an Agilent 6520 QTOF mass spectrometer. Peak area ratio of the analyte to the internal standard was plotted against a **14** standard curve to yield **14** concentrations for each sample.

Pharmacokinetic and Statistical Analysis

Area under the curve (AUC) was calculated by log-linear trapezoidal rule to the end of sample collection by noncompartmental analysis module in WinNonlin (version 5.3, Certara, St. Louis, MO). cLogPs were calculated using ChemDraw Professional (PerkinElmer, Waltham, MA). The half-life ($t_{1/2}$) of prodrug metabolic stability from brain homogenates was estimated using the first-order equation $t_{1/2} = 0.693/K_{el}$, where K_{el} (elimination rate constant) is the slope of linear regression from natural log percentage substrate remaining versus incubation time.[75] For all studies, group means and standard errors were calculated and used for statistical comparisons where appropriate. Differences in radial arm water maze errors and latencies between groups were assessed by two-way ANOVA (treatment × trial) with posthoc Tukey test. Viral load in each tissue was compared between treatment groups by *t* test. Prodrug half-lives were compared by one-way ANOVA. For all tests, significance was defined as $p < 0.05$.

Supplementary Material

Refer to Web version on PubMed Central for supplementary material.

ABBREVIATIONS

DON	6-diazo-5-oxo-L-norleucine
HAND	HIV-associated neurocognitive disorders
cART	combined antiretroviral therapy
HAD	HIV-associated dementia
CNS	central nervous system
MRS	magnetic resonance spectroscopy
CSF	cerebrospinal fluid
GI	gastrointestinal
cLogP	calculated partition coefficient
DCM	dichloromethane
DMF	dimethylformamide
RAWM	radial arm water maze
LT	learning trial
RT	retention trial
AUC	area under the curve
POM	pivaloyloxymethyl

ELISA	enzyme-linked immunosorbent assay
pi	post-inoculation
iv	intravenous
ip	intraperitoneal
qPCR	quantitative polymerase chain reaction
CVC	central venous catheter
LC	liquid chromotagraphy
MS	mass spectrometry
ESI	electrospray ionization

References

1. Zink MC. Translational research models and novel adjunctive therapies for neuroAIDS. J Neuroimmune Pharmacol. 2007; 2:14–19. [PubMed: 18040821]
2. Heaton RK, Clifford DB, Franklin DR Jr, Woods SP, Ake C, Vaida F, Ellis RJ, Letendre SL, Marcotte TD, Atkinson JH, Rivera-Mindt M, Vigil OR, Taylor MJ, Collier AC, Marra CM, Gelman BB, McArthur JC, Morgello S, Simpson DM, McCutchan JA, Abramson I, Gamst A, Fennema-Notestine C, Jernigan TL, Wong J, Grant I. HIV-associated neurocognitive disorders persist in the era of potent antiretroviral therapy: CHARTER Study. Neurology. 2010; 75:2087–2096. [PubMed: 21135382]
3. Harezlak J, Buchthal S, Taylor M, Schifitto G, Zhong J, Daar E, Alger J, Singer E, Campbell T, Yiannoutsos C, Cohen R, Navia B. Persistence of HIV-associated cognitive impairment, inflammation, and neuronal injury in era of highly active antiretroviral treatment. AIDS. 2011; 25:625–633. [PubMed: 21297425]
4. Heaton RK, Franklin DR, Ellis RJ, McCutchan JA, Letendre SL, Leblanc S, Corkran SH, Duarte NA, Clifford DB, Woods SP, Collier AC, Marra CM, Morgello S, Mindt MR, Taylor MJ, Marcotte TD, Atkinson JH, Wolfson T, Gelman BB, McArthur JC, Simpson DM, Abramson I, Gamst A, Fennema-Notestine C, Jernigan TL, Wong J, Grant I. HIV-associated neurocognitive disorders before and during the era of combination antiretroviral therapy: differences in rates, nature, and predictors. J NeuroVirol. 2011; 17:3–16. [PubMed: 21174240]
5. Robertson KR, Smurzynski M, Parsons TD, Wu K, Bosch RJ, Wu J, McArthur JC, Collier AC, Evans SR, Ellis RJ. The prevalence and incidence of neurocognitive impairment in the HAART era. AIDS. 2007; 21:1915–1921. [PubMed: 17721099]
6. Potter MC, Figuera-Losada M, Rojas C, Slusher BS. Targeting the glutamatergic system for the treatment of HIV-associated neurocognitive disorders. J Neuroimmune Pharmacol. 2013; 8:594–607. [PubMed: 23553365]
7. Vazquez-Santiago FJ, Noel RJ Jr, Porter JT, Rivera-Amill V. Glutamate metabolism and HIV-associated neurocognitive disorders. J NeuroVirol. 2014; 20:315–331. [PubMed: 24867611]
8. Doi A, Iijima K, Kano S, Ishizaka Y. Viral protein R of HIV type-1 induces retrotransposition and upregulates glutamate synthesis by the signal transducer and activator of transcription 1 signaling pathway. Microbiol Immunol. 2015; 59:398–409. [PubMed: 25990091]
9. Erdmann N, Tian C, Huang Y, Zhao J, Herek S, Curthoys N, Zheng J. In vitro glutaminase regulation and mechanisms of glutamate generation in HIV-1-infected macrophage. J Neurochem. 2009; 109:551–561. [PubMed: 19222703]
10. Erdmann N, Zhao J, Lopez AL, Herek S, Curthoys N, Hexum TD, Tsukamoto T, Ferraris D, Zheng J. Glutamate production by HIV-1 infected human macrophage is blocked by the inhibition of glutaminase. J Neurochem. 2007; 102:539–549. [PubMed: 17596215]

11. Erdmann NB, Whitney NP, Zheng J. Potentiation of excitotoxicity in HIV-1 associated dementia and the significance of glutaminase. Clin Neurosci Res. 2006; 6:315–328. [PubMed: 18059978]
12. Huang Y, Zhao L, Jia B, Wu L, Li Y, Curthoys N, Zheng JC. Glutaminase dysregulation in HIV-1-infected human microglia mediates neurotoxicity: relevant to HIV-1-associated neurocognitive disorders. J Neurosci. 2011; 31:15195–15204. [PubMed: 22016553]
13. Thomas AG, O'Driscoll CM, Bressler J, Kaufmann W, Rojas CJ, Slusher BS. Small molecule glutaminase inhibitors block glutamate release from stimulated microglia. Biochem Biophys Res Commun. 2014; 443:32–36. [PubMed: 24269238]
14. Tian C, Erdmann N, Zhao J, Cao Z, Peng H, Zheng J. HIV-infected macrophages mediate neuronal apoptosis through mitochondrial glutaminase. J Neurochem. 2008; 105:994–1005. [PubMed: 18088378]
15. Tian C, Sun L, Jia B, Ma K, Curthoys N, Ding J, Zheng J. Mitochondrial glutaminase release contributes to glutamate-mediated neurotoxicity during human immunodeficiency virus-1 infection. J Neuroimmune Pharmacol. 2012; 7:619–628. [PubMed: 22527635]
16. Wu B, Huang Y, Braun AL, Tong Z, Zhao R, Li Y, Liu F, Zheng JC. Glutaminase-containing microvesicles from HIV-1-infected macrophages and immune-activated microglia induce neurotoxicity. Mol Neurodegener. 2015; 10:61. [PubMed: 26546362]
17. Ye L, Huang Y, Zhao L, Li Y, Sun L, Zhou Y, Qian G, Zheng JC. IL-1beta and TNF-alpha induce neurotoxicity through glutamate production: a potential role for neuronal glutaminase. J Neurochem. 2013; 125:897–908. [PubMed: 23578284]
18. Zhao L, Huang Y, Tian C, Taylor L, Curthoys N, Wang Y, Vernon H, Zheng J. Interferon-alpha regulates glutaminase 1 promoter through STAT1 phosphorylation: relevance to HIV-1 associated neurocognitive disorders. PLoS One. 2012; 7:e32995. [PubMed: 22479354]
19. Zhao L, Huang Y, Zheng J. STAT1 regulates human glutaminase 1 promoter activity through multiple binding sites in HIV-1 infected macrophages. PLoS One. 2013; 8:e76581. [PubMed: 24086752]
20. Musante V, Summa M, Neri E, Puliti A, Godowicz TT, Severi P, Battaglia G, Raiteri M, Pittaluga A. The HIV-1 viral protein Tat increases glutamate and decreases GABA exocytosis from human and mouse neocortical nerve endings. Cereb Cortex. 2010; 20:1974–1984. [PubMed: 20034999]
21. Anderson ER, Boyle J, Zink WE, Persidsky Y, Gendelman HE, Xiong H. Hippocampal synaptic dysfunction in a murine model of human immunodeficiency virus type 1 encephalitis. Neuroscience. 2003; 118:359–369. [PubMed: 12699772]
22. Anderson ER, Gendelman HE, Xiong H. Memantine protects hippocampal neuronal function in murine human immunodeficiency virus type 1 encephalitis. J Neurosci. 2004; 24:7194–7198. [PubMed: 15306653]
23. Behnisch T, Francesconi W, Sanna PP. HIV secreted protein Tat prevents long-term potentiation in the hippocampal CA1 region. Brain Res. 2004; 1012:187–189. [PubMed: 15158177]
24. Dong J, Xiong H. Human immunodeficiency virus type 1 gp120 inhibits long-term potentiation via chemokine receptor CXCR4 in rat hippocampal slices. J Neurosci Res. 2006; 83:489–496. [PubMed: 16400660]
25. Fitting S, Ignatowska-Jankowska BM, Bull C, Skoff RP, Lichtman AH, Wise LE, Fox MA, Su J, Medina AE, Krahe TE, Knapp PE, Guido W, Hauser KF. Synaptic dysfunction in the hippocampus accompanies learning and memory deficits in human immunodeficiency virus type-1 Tat transgenic mice. Biol Psychiatry. 2013; 73:443–453. [PubMed: 23218253]
26. Keblesh JP, Dou H, Gendelman HE, Xiong H. 4-Aminopyridine improves spatial memory in a murine model of HIV-1 encephalitis. J Neuroimmune Pharmacol. 2009; 4:317–327. [PubMed: 19462247]
27. Li ST, Matsushita M, Moriwaki A, Saheki Y, Lu YF, Tomizawa K, Wu HY, Terada H, Matsui H. HIV-1 Tat inhibits long-term potentiation and attenuates spatial learning [corrected]. Ann Neurol. 2004; 55:362–371. [PubMed: 14991814]
28. Tang H, Lu D, Pan R, Qin X, Xiong H, Dong J. Curcumin improves spatial memory impairment induced by human immunodeficiency virus type 1 glycoprotein 120 V3 loop peptide in rats. Life Sci. 2009; 85:1–10. [PubMed: 19345695]

29. Cassol E, Misra V, Dutta A, Morgello S, Gabuzda D. Cerebrospinal fluid metabolomics reveals altered waste clearance and accelerated aging in HIV patients with neurocognitive impairment. AIDS. 2014; 28:1579–1591. [PubMed: 24752083]
30. Bairwa D, Kumar V, Vyas S, Das BK, Srivastava AK, Pandey RM, Sharma SK, Jagannathan NR, Sinha S. Case control study: magnetic resonance spectroscopy of brain in HIV infected patients. BMC Neurol. 2016; 16:99. [PubMed: 27405321]
31. Ernst T, Jiang CS, Nakama H, Buchthal S, Chang L. Lower brain glutamate is associated with cognitive deficits in HIV patients: a new mechanism for HIV-associated neurocognitive disorder. J Magn Reson Imaging. 2010; 32:1045–1053. [PubMed: 21031507]
32. Mohamed MA, Barker PB, Skolasky RL, Selnes OA, Moxley RT, Pomper MG, Sacktor NC. Brain metabolism and cognitive impairment in HIV infection: a 3-T magnetic resonance spectroscopy study. Magn Reson Imaging. 2010; 28:1251–1257. [PubMed: 20688449]
33. Sailasuta N, Shriner K, Ross B. Evidence of reduced glutamate in the frontal lobe of HIV-seropositive patients. NMR Biomed. 2009; 22:326–331. [PubMed: 18988228]
34. Schifitto G, Navia BA, Yiannoutsos CT, Marra CM, Chang L, Ernst T, Jarvik JG, Miller EN, Singer EJ, Ellis RJ, Kolson DL, Simpson D, Nath A, Berger J, Shriver SL, Millar LL, Colquhoun D, Lenkinski R, Gonzalez RG, Lipton SA. Memantine and HIV-associated cognitive impairment: a neuropsychological and proton magnetic resonance spectroscopy study. AIDS. 2007; 21:1877–1886. [PubMed: 17721095]
35. Stankoff B, Tourbah A, Suarez S, Turell E, Stievenart JL, Payan C, Coutellier A, Herson S, Baril L, Bricaire F, Calvez V, Cabanis EA, Lacomblez L, Lubetzki C. Clinical and spectroscopic improvement in HIV-associated cognitive impairment. Neurology. 2001; 56:112–115. [PubMed: 11148248]
36. Gelman BB, Chen T, Lisinicchia JG, Soukup VM, Carmical JR, Starkey JM, Masliah E, Commins DL, Brandt D, Grant I, Singer EJ, Levine AJ, Miller J, Winkler JM, Fox HS, Luxon BA, Morgello S. The National NeuroAIDS Tissue Consortium brain gene array: two types of HIV-associated neurocognitive impairment. PLoS One. 2012; 7:e46178. [PubMed: 23049970]
37. Gelman BB, Lisinicchia JG, Chen T, Johnson KM, Jennings K, Freeman DH Jr, Soukup VM. Prefrontal dopaminergic and enkephalinergic synaptic accommodation in HIV-associated neurocognitive disorders and encephalitis. J Neuroimmune Pharmacol. 2012; 7:686–700. [PubMed: 22391864]
38. Borjabad A, Morgello S, Chao W, Kim SY, Brooks AI, Murray J, Potash MJ, Volsky DJ. Significant effects of antiretroviral therapy on global gene expression in brain tissues of patients with HIV-1-associated neurocognitive disorders. PLoS Pathog. 2011; 7:e1002213. [PubMed: 21909266]
39. Conti F, Minelli A. Glutamate immunoreactivity in rat cerebral cortex is reversibly abolished by 6-diazo-5-oxo-L-norleucine (DON), an inhibitor of phosphate-activated glutaminase. J Histochem Cytochem. 1994; 42:717–726. [PubMed: 7910617]
40. Chung SH, Johnson MS. Studies on sound-induced epilepsy in mice. Proc R Soc London, Ser B. 1984; 221:145–168. [PubMed: 6145159]
41. Zhao J, Lopez AL, Erichsen D, Herek S, Cotter RL, Curthoys NP, Zheng J. Mitochondrial glutaminase enhances extracellular glutamate production in HIV-1-infected macrophages: linkage to HIV-1 associated dementia. J Neurochem. 2004; 88:169–180. [PubMed: 14675161]
42. Potash MJ, Chao W, Bentsman G, Paris N, Saini M, Nitkiewicz J, Belem P, Sharer L, Brooks AI, Volsky DJ. A mouse model for study of systemic HIV-1 infection, antiviral immune responses, and neuroinvasiveness. Proc Natl Acad Sci U S A. 2005; 102:3760–3765. [PubMed: 15728729]
43. He H, Sharer LR, Chao W, Gu CJ, Borjabad A, Hadas E, Kelschenbach J, Ichiyama K, Do M, Potash MJ, Volsky DJ. Enhanced human immunodeficiency virus Type 1 expression and neuropathogenesis in knockout mice lacking Type I interferon responses. J Neuropathol Exp Neurol. 2014; 73:59–71. [PubMed: 24335529]
44. Earhart RH, Amato DJ, Chang AY, Borden EC, Shiraki M, Dowd ME, Comis RL, Davis TE, Smith TJ. Phase II trial of 6-diazo-5-oxo-L-norleucine versus aclacinomycin-A in advanced sarcomas and mesotheliomas. Invest New Drugs. 1990; 8:113–119. [PubMed: 2188926]

45. Magill GB, Myers WP, Reilly HC, Putnam RC, Magill JW, Sykes MP, Escher GC, Karnofsky DA, Burchenal JH. Pharmacological and initial therapeutic observations on 6-diazo-5-oxo-1-norleucine (DON) in human neoplastic disease. Cancer. 1957; 10:1138–1150. [PubMed: 13489662]
46. Rahman A, Smith FP, Luc PT, Woolley PV. Phase I study and clinical pharmacology of 6-diazo-5-oxo-L-norleucine (DON). Invest New Drugs. 1985; 3:369–374. [PubMed: 4086244]
47. Rais R, Jancarik A, Tenora L, Nedelcovych M, Alt J, Englert J, Rojas C, Le A, Elgogary A, Tan J, Monincova L, Pate K, Adams R, Ferraris D, Powell J, Majer P, Slusher BS. Discovery of 6-Diazo-5-oxo-l-norleucine (DON) prodrugs with enhanced CSF delivery in monkeys: a potential treatment for glioblastoma. J Med Chem. 2016; 59:8621–8633. [PubMed: 27560860]
48. Rasheed A, Kumar CKA. Novel approaches on prodrug based drug design. Pharm Chem J. 2008; 42:677–686.
49. Li F, Maag H, Alfredson T. Prodrugs of nucleoside analogues for improved oral absorption and tissue targeting. J Pharm Sci. 2008; 97:1109–1134. [PubMed: 17696166]
50. Fattash, B., Karaman, R. Chemical approaches used in prodrugs design. In: Karaman, R., editor. Prodrugs Design – A New Era ; Pharmacology—Research, Safety Testing and Regulation. Nova Science Publishers Inc.; New York: 2014. p. 103-138.
51. Liederer BM, Borchardt RT. Enzymes involved in the bioconversion of ester-based prodrugs. J Pharm Sci. 2006; 95:1177–1195. [PubMed: 16639719]
52. Rautio J, Laine K, Gynther M, Savolainen J. Prodrug approaches for CNS delivery. AAPS J. 2008; 10:92–102. [PubMed: 18446509]
53. Vlieghe P, Khrestchatisky M. Medicinal chemistry based approaches and nanotechnology-based systems to improve CNS drug targeting and delivery. Med Res Rev. 2013; 33:457–516. [PubMed: 22434495]
54. Fu J, Pacyniak E, Leed MGD, Sadgrove MP, Marson L, Jay M. Interspecies differences in the metabolism of a multiester prodrug by carboxylesterases. J Pharm Sci. 2016; 105:989–995. [PubMed: 26344572]
55. Van Gelder J, Shafiee M, De Clercq E, Penninckx F, Van den Mooter G, Kinget R, Augustijns P. Species-dependent and site-specific intestinal metabolism of ester prodrugs. Int J Pharm. 2000; 205:93–100. [PubMed: 11000545]
56. Suenderhauf C, Parrott N. A physiologically based pharmacokinetic model of the minipig: data compilation and model implementation. *Pharm.* Res. 2013; 30:1–15.
57. Gallop MA, Yao F, Ludwikow MJ, Phan T, Peng G. Acyloxyalkyl Carbamate Prodrugs, Methods of Synthesis and Use. WO Pat Appl. 2005; 2005019163:A2.
58. Gallop MA, Xu F, Phan T, Dilip U, Peng G. Acyloxyalkyl Carbamate Prodrugs, Methods of Synthesis and Use. WO Pat Appl. 2008; 2008033572:A1.
59. Gallop M, Cundy K, Zhou C, Yao F, Xiang JN, Ollman I, Qiu F. Prodrugs of GABA Analogs, Compositions and Uses Thereof. US Pat Appl. 2006; 29361:A1. 2006/02.
60. Woods SP, Moore DJ, Weber E, Grant I. Cognitive neuropsychology of HIV-associated neurocognitive disorders. Neuropsychol Rev. 2009; 19:152–168. [PubMed: 19462243]
61. Lee CF, Lo YC, Cheng CH, Furtmuller GJ, Oh B, Andrade-Oliveira V, Thomas AG, Bowman CE, Slusher BS, Wolfgang MJ, Brandacher G, Powell JD. Preventing allograft rejection by targeting immune metabolism. Cell Rep. 2015; 13:760–770. [PubMed: 26489460]
62. Baxter VK, Glowinski R, Braxton AM, Potter MC, Slusher BS, Griffin DE. Glutamine antagonist-mediated immune suppression decreases pathology but delays virus clearance in mice during nonfatal alphavirus encephalomyelitis. Virology. 2017; 508:134–149. [PubMed: 28531865]
63. Annaert P, Tukker JJ, van GelderJ, Naesens L, de ClercqE, van DenMooter G, Kinget R, Augustijns P. In vitro, ex vivo, and in situ intestinal absorption characteristics of the antiviral ester prodrug adefovir dipivoxil. J Pharm Sci. 2000; 89:1054–1062. [PubMed: 10906729]
64. Masuda K, Naiki M. Method for Promoting the Synthesis of Collagen and Proteoglycan in Chondrocytes. US Pat Appl. 2013; 64383:A1. 2013/01.
65. Potash MJ, Chao W, Bentsman G, Paris N, Saini M, Nitkiewicz J, Belem P, Sharer L, Brooks AI, Volsky DJ. A mouse model for study of systemic HIV-1 infection, antiviral immune responses, and neuroinvasiveness. Proc Natl Acad Sci U S A. 2005; 102:3760–3765. [PubMed: 15728729]

66. Shijie J, Takeuchi H, Yawata I, Harada Y, Sonobe Y, Doi Y, Liang J, Hua L, Yasuoka S, Zhou Y, Noda M, Kawanokuchi J, Mizuno T, Suzumura A. Blockade of glutamate release from microglia attenuates experimental autoimmune encephalomyelitis in mice. Tohoku J Exp Med. 2009; 217:87–92. [PubMed: 19212100]

67. Manivannan S, Baxter VK, Schultz KL, Slusher BS, Griffin DE. Protective Effects of Glutamine Antagonist 6-Diazo-5-Oxo-l-Norleucine in Mice with Alphavirus Encephalomyelitis. J Virol. 2016; 90:9251–9262. [PubMed: 27489275]

68. Potter MC, Baxter VK, Mathey RW, Alt J, Rojas C, Griffin DE, Slusher BS. Neurological sequelae induced by alphavirus infection of the CNS are attenuated by treatment with the glutamine antagonist 6-diazo-5-oxo-l-norleucine. J NeuroVirol. 2015; 21:159–173. [PubMed: 25645378]

69. Alt J, Potter MC, Rojas C, Slusher BS. Bioanalysis of 6-diazo-5-oxo-l-norleucine in plasma and brain by ultra-performance liquid chromatography mass spectrometry. Biochem. 2015; 474:28–34.

70. Arendash GW, Gordon MN, Diamond DM, Austin LA, Hatcher JM, Jantzen P, DiCarlo G, Wilcock D, Morgan D. Behavioral assessment of Alzheimer's transgenic mice following long-term Abeta vaccination: task specificity and correlations between Abeta deposition and spatial memory. DNA Cell Biol. 2001; 20:737–744. [PubMed: 11788052]

71. Hadas E, Borjabad A, Chao W, Saini M, Ichiyama K, Potash MJ, Volsky DJ. Testing antiretroviral drug efficacy in conventional mice infected with chimeric HIV-1. AIDS. 2007; 21:905–909. [PubMed: 17457083]

72. He H, Sharer LR, Chao W, Gu CJ, Borjabad A, Hadas E, Kelschenbach J, Ichiyama K, Do M, Potash MJ, Volsky DJ. Enhanced human immunodeficiency virus type 1 expression and neuropathogenesis in knockout mice lacking type I interferon responses. J Neuropathol Exp Neurol. 2014; 73:59–71. [PubMed: 24335529]

73. Kelschenbach JL, Saini M, Hadas E, Gu C-J, Chao W, Bentsman G, Hong JP, Hanke T, Sharer LR, Potash MJ, Volsky DJ. Mice chronically infected with chimeric HIV resist peripheral and brain superinfection: A model of protective immunity to HIV. J Neuroimmune Pharmacol. 2012; 7:380–387. [PubMed: 21987348]

74. Rais R, Hoover R, Wozniak K, Rudek MA, Tsukamoto T, Alt J, Rojas C, Slusher BS. Reversible disulfide formation of the glutamate carboxypeptidase II inhibitor E2072 results in prolonged systemic exposures in vivo. Drug Metab. Dispos. 2012; 40:2315–2323.

75. Baranczewski P, Stanczak A, Sundberg K, Svensson R, Wallin A, Jansson J, Garberg P, Postlind H. Introduction to in vitro estimation of metabolic stability and drug interactions of new chemical entities in drug discovery and development. Pharmacol Rep. 2006; 58:453–472. [PubMed: 16963792]

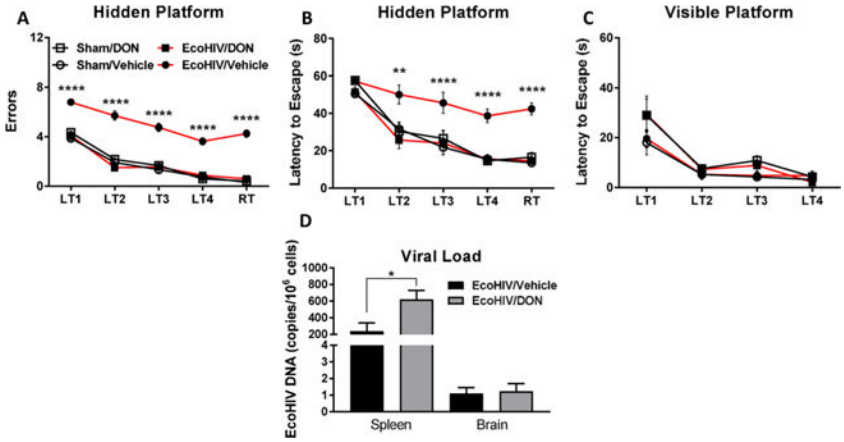

Figure 1.

DON (**14**) prevented cognitive decline in the EcoHIV model of HAND. DON (**14**) treatment (1 mg/kg, ip) was begun prior to EcoHIV inoculation and continued every other day throughout the 30 day infection period and during radial arm water maze (RAWM) testing. **14** significantly attenuated spatial learning and memory deficits in the RAWM as measured by (A) number of errors across learning trials (LT) 1–4 and the retention trial (RT) and (B) latency to escape to a hidden platform relative to sham-inoculated control mice. **14** had no effect on (C) RAWM escape latency to a visible platform. **14** treatment also caused (D) a slight increase in EcoHIV viral load as measured by DNA copies in the spleen but had no effect on viral load in the brain. Behavioral comparison conducted by two-way ANOVA, posthoc comparison by Tukey's test; ****$p < 0.0001$, EcoHIV/Veh vs Sham/Veh, EcoHIV/DON, and Sham/DON. Viral load comparison conducted by t test, *$p < 0.05$, $n = 8$/group.

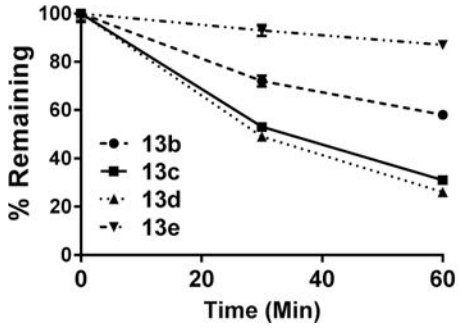

Compound	$t_{1/2}$ ± SEM
13b	75 ± 2
13c	35 ± 2
13d	31 ± 1
13e	291 ± 44

Figure 2.

N-(Pivaloyloxy)alkoxy-carbonyl prodrugs of DON (**14**) showed differential rates of metabolism in swine brain homogenate. Compounds **13b**–**e** (10 μM) were spiked into swine brain homogenate (1% w/v); concentrations of the prodrug remaining were measured by LC-MS/MS at 0, 30, or 60 min post incubation. The prodrugs were metabolized at varying rates, with **13c** and **13d** showing the highest lability. Data are depicted as mean ± SEM. Half-lives ($t_{1/2}$) compared by one-way ANOVA, $p < 0.0001$, $n = 3$/group.

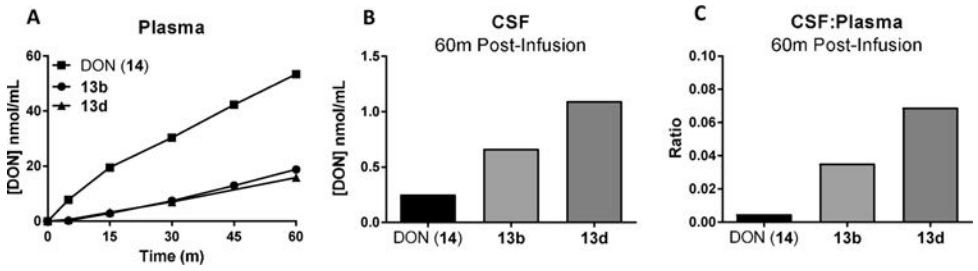

Figure 3.

In vivo pharmacokinetics of DON following iv administration of DON (**14**), **13b**, and **13d** in swine plasma and CSF. DON (**14**, 1.6 mg/kg, iv) or an equivalent dose of either **13b** or **13d** were administered to swine. Plasma (0–60 min) and CSF (60 min) concentrations of **14** were evaluated via LC-MS/MS. Relative to **14**, compounds **13b** or **13d** delivered (A) lower **14** plasma exposure and (B) higher **14** CSF concentrations, resulting in (C) more than 7-fold or 15-fold enhanced CSF:plasma ratio at 60 min postadministration, respectively.

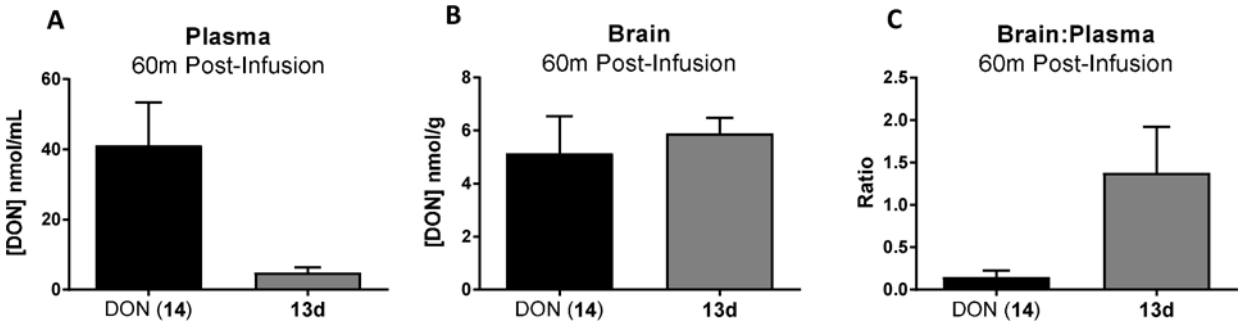

Figure 4.

In vivo pharmacokinetics of DON following iv administration of DON (**14**) and **13d** in swine plasma and brain. DON (**14**, 1.6 mg/kg, iv) or an equivalent dose of **13d** was administered to swine. Swine were sacrificed, and plasma and brain (60 min) concentrations of **14** were evaluated via LC-MS/MS. Relative to **14**, compound **13d** delivered (A) lower **14** plasma concentrations and (B) comparable **14** brain concentrations, resulting in (C) a 9-fold enhanced brain:plasma ratio at 60 min postadministration. Data are depicted as mean ± SEM (n = 2/group). Free levels of **14** in the swine brain (F_b = 91%) were calculated to be 0.46 and 0.53 nmol/g following **14** and **13d** administration, respectively.

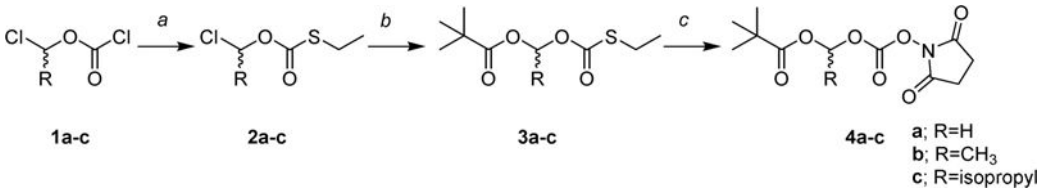

Scheme 1. Synthesis of *N*-Hydroxysuccinimide Esters of Pivaloyloxy-alkoxycarbonates Intermediates 4a–c[a]

[a]Reagents and conditions: (a) EtSH, Et_3N, Et_2O, 0 °C to rt, 17–25 h; (b) pivalic acid, DIPEA, 60–70 °C, 20–70 h; (c) *N*-hydroxysuccinimide, peracetic acid, DCM, 0 °C to rt, 3 h.

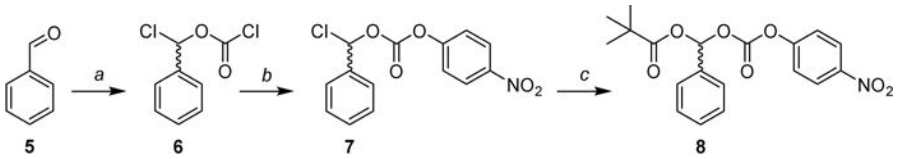

Scheme 2. Synthesis of 4-Nitrophenyl Esters of Pivaloyloxy-alkoxycarbonate Intermediate 8[a]

[a]Reagents and conditions: (a) triphosgene, pyridine, Et_2O, –20 °C to rt, 20 h; (b) 4-nitrophenol, pyridine, DCM, 0 °C to rt, 2 h; (c) $Hg(OPiv)_2$, DCM, rt, 16 h.

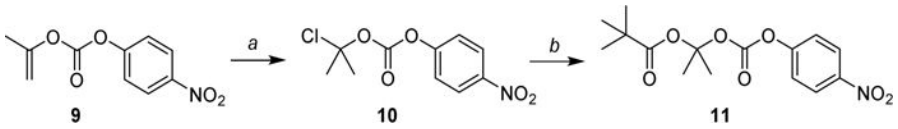

Scheme 3. Synthesis of Intermediate 11[a]

[a]Reagents and conditions: (a) 4 M HCl, dioxane, rt, 21 h; (b) $Hg(OPiv)_2$, DCM, rt, 20 h.

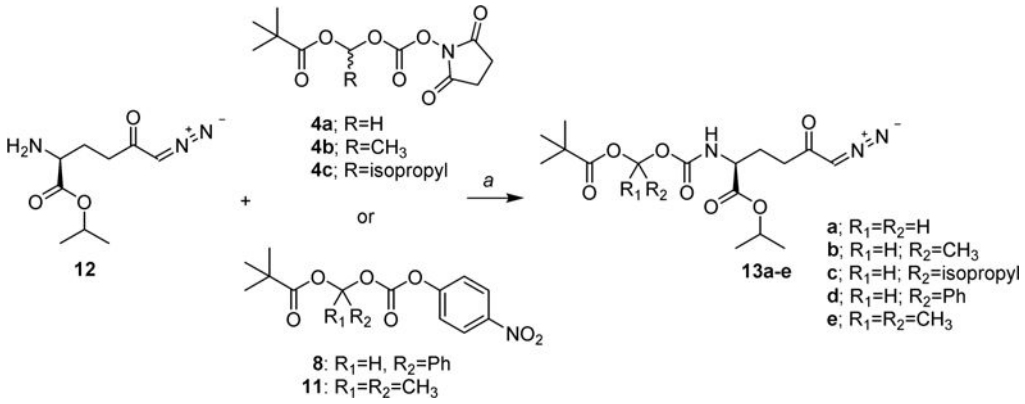

Scheme 4. Synthesis of 14 Prodrugs 13a –e[a]

[a]Reagents and conditions: (a) DCM or DMF, 0 °C to rt, 2–5 h.

Table 1

Lipophilicity and Stability of *N*-(Pivaloyloxy)alkoxy-carbonyl Prodrugs of DON (14)

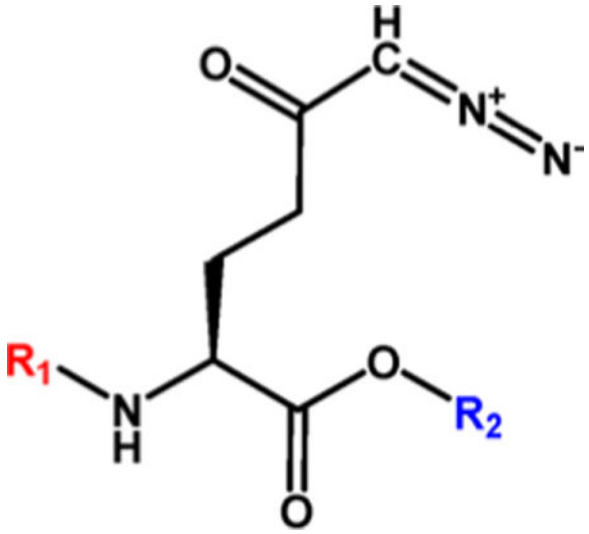

Cmpd	R_1	R_2	cLogP	Plasma Stability (*% remainin at 60 min*)			Brain Stability (*% remaining at 60 min*)
				Mouse	*Human*	*Swine*	*Swine*
14	H	H	−2.50	–	–	–	–
13a	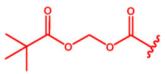		1.19	0	9[47]	–	–
13b	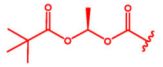		1.50	0	91[47]	86±5	58±1
13c	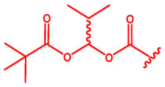		2.42	0	100±7	100±3	31±1

Cmpd	R_1	R_2	cLogP	Plasma Stability (% remainin at 60 min)			Brain Stability (% remaining at 60 min)
				Mouse	*Human*	*Swine*	*Swine*
13d			2.75	0	88±5	83±1	26±0
13e			1.81	0	93±5	85±3	87±2

Table 2

Total and Free DON (14) Concentrations 60 min Post-Administration of 14 or 13d in Swine (1.6 mg/kg Equivalent, iv)

	brain (nmol/g)		plasma (nmol/mL)		CSF (nmol/mL)
	total	free	total	free	total
14	5.15 ± 1.40	0.464 ± 0.126	41.2 ± 12.2	32.5 ± 9.64	0.252
13d	5.90 ± 0.590	0.531 ± 0.053	4.88 ± 1.50	3.86 ± 1.19	1.10

Table 3

Total and Free DON (14) Ratios 60 min Post-Administration of 14 or 13d in Swine (1.6 mg/kg Equivalent, iv)

	brain:plasma		CSF:plasma		CSF:brain
	total:total	free:free	total:total	total:free	total:free
14	0.148 ± 0.078	0.017 ± 0.001	0.005	0.006	0.543
13d	1.38 ± 0.544	0.157 ± 0.062	0.069	0.087	2.07